

Fuzzy logic controlled Doubly Fed Induction Generator (DFIG) for Wind Energy Conversion System using MATLAB

M.BHANU PRAKASH¹ T.MADHURANTHAKA²

¹P.G. Student, Department of EEE, S.V. College of Engineering, Tirupati, A.P., INDIA.

²HOD, Department of EEE, S.V. College of Engineering, Tirupati, A.P., INDIA.

ABSTRACT: This paper presents the operation of doubly fed induction generator (DFIG) with Fuzzy Logic Control & an integrated active filter capabilities using grid-side converter (GSC). The main contribution of this work lies in the control of GSC using Fuzzy Logic Control (FLC) for supplying harmonics in addition to its slip power transfer. The rotor-side converter (RSC) is used for attaining maximum power extraction and to supply required reactive power to DFIG. This wind energy conversion system (WECS) works as a static compensator (STATCOM) for supplying harmonics even when the wind turbine is in shutdown condition. Control algorithms of both GSC and RSC are presented in detail. The proposed FLC based DFIG-based WECS is simulated using MATLAB/Simulink. A prototype of the proposed FLCDFIG based WECS is developed in MATLAB/SIMULINK environment. Simulated results are validated with test results of the developed FLC based DFIG for different practical conditions, such as variable wind speed and unbalanced/single phase loads.

KEYWORDS: Fuzzy Logic Controller (FLC), Doubly fed induction generator (DFIG), integrated active filter, nonlinear load, power quality, wind energy conversion system (WECS).

I. INTRODUCTION

With the increase in population and industrialization, the energy demand has increased significantly. However, the conventional energy sources such as coal, oil, and gas are limited in nature. Now, there is a need for renewable energy sources for the future energy demand [1]. The other main advantages of this renewable source are eco-friendliness and unlimited in nature [2]. Due to technical advancements, the cost of the wind power produced is comparable to that of conventional power plants. Therefore, the wind energy is the most preferred out of all renewable energy sources [3]. In the initial days, wind turbines have been used as fixed speed wind turbines with squirrel cage induction generator and capacitor banks. Most of the wind turbines are fixed speed because of their simplicity and low cost [4]. By observing wind turbine characteristics, one can clearly identify that for extracting maximum power, the machine should run at varying rotor speeds at different wind speeds. Using modern power electronic converters, the machine is able to run at adjustable speeds [5]. Therefore, these variable speed wind turbines are able to improve the wind energy production [6]. Out of all variable speed wind turbines, doubly fed induction generators (DFIGs) are preferred because of their low cost [7]. The other advantages of this DFIG are the higher energy output, lower converter rating, and better utilization of generators [8]. These DFIGs also provide good damping performance for the weak grid [9]. Independent control of active and reactive power is achieved by the decoupled vector control algorithm presented in [10] and [11]. This vector control of such system is usually realized in synchronously rotating reference frame oriented in either voltage axis or flux axis. In this work, the control of rotor-side converter (RSC) is implemented in voltage-oriented reference frame. Grid code requirements for the grid connection and operation of wind farms are discussed in [12]. Response of DFIG-based [35] Current distortion limits for general distribution systems in terms of individual harmonic order (odd harmonics) [35].

TABLE I

I_h/I_L	<11	11 ≤ h ≤ 17	17 ≤ h ≤ 23	23 ≤ h ≤ 35	35 ≤ h	TDD
<20	4.0	2.0	1.5	0.6	0.3	5.0
20 < 50	7.0	3.5	2.5	1.0	0.5	8.0
50 < 100	10	4.5	4.0	1.5	0.7	12
100 < 1000	12	5.5	5.0	2.0	1.0	15.0
> 1000	15.0	7.0	6.0	2.5	1.4	20.0

Maximum harmonic current distortion is in percent of $IL.sc$ = maximum short-circuit current at PCC; IL = maximum demand load current (fundamental frequency component) at PCC.

Wind energy conversion system (WECS) to grid disturbance's compared to the fixed speed WECS in [13]. As the wind penetration in the grid becomes significant, the use of variable speed WECS for supplementary jobs such as power smoothing and harmonic mitigation are compulsory in addition to its power generation. This power smoothing is achieved by including super magnetic energy storage systems as proposed in [14]. The other auxiliary services such as reactive power requirement and transient stability limit are achieved by including static compensator (STATCOM) in [15]. A distribution STATCOM (DSTATCOM) coupled with fly-wheel energy storage system is used at the wind farm for mitigating harmonics and frequency disturbances [16]. However, the authors have used two more extra converters for this purpose. A super capacitor energy storage system at the dc link of unified power quality conditioner (UPQC) is proposed in [17] for improving power quality and reliability. In all above methods [15]–[17], the authors have used separate converters for compensating the harmonics and also for controlling the reactive power. However, in later stages, some of the researchers have modified the control algorithms of already existed DFIG converters for mitigating the power quality problems and reactive power compensation [18]–[26]. The harmonics compensation and reactive power control are achieved with the help of existing RSC [18]–[23]. Therefore, harmonics are injected from the RSC into the rotor windings. This creates losses and noise in the machine. These different harmonics in rotating part may also create mechanical unbalance. Moreover, both reactive power compensation and harmonic compensation are achieved in all these methods using RSC control. These methods increase the RSC rating. In [24] and [25], harmonic compensation and reactive power control are done using GSC. Therefore, the harmonics are not passing through machine windings in all these cases. Todeschini and Emanuel [26] have compared three different control algorithms and finally concluded that combined modulation of both RSC and GSC are needed for compensating the harmonics and controlling the reactive power. However, the authors have used direct current control of GSC. Therefore, harmonic compensation is not so effective and total harmonic distortion (THD) is not less than 5% as per IEEE-519 standard given in Table I. The authors have also not verified simulation results experimentally. An indirect current control technique is simple and shows better performance for eliminating harmonics as compared to direct current control [27]–[30]. In this work, a new control algorithm for GSC is proposed for compensating harmonics produced by nonlinear loads using an indirect current control. RSC is used for controlling the reactive power of DFIG. The other main advantage of proposed DFIG is that it works as an active filter even when the wind turbine is in shutdown condition. Therefore, it compensates load reactive power and harmonics at wind turbine stalling case. Both simulation and experimental performances of the proposed integrated active filter-based DFIG are presented in this work. The dynamic performance of the proposed DFIG is also demonstrated for varying wind speeds and changes in unbalanced nonlinear loads at point of common coupling (PCC).

II. SYSTEM CONFIGURATION AND OPERATING PRINCIPLE

Fig. 1 shows a schematic diagram of the proposed DFIG based WECS with integrated active filter capabilities. In DFIG, the stator is directly connected to the grid as shown in Fig. 1. Two back-to-back connected voltage source converters (VSCs) are placed between the rotor and the grid. Nonlinear loads are connected at PCC as shown in Fig. 1. The proposed DFIG works as an active filter in addition to the active power generation similar to normal DFIG. Harmonics generated by the nonlinear load connected at the PCC distort the PCC voltage. These nonlinear load harmonic currents are mitigated by GSC control, so that the stator and grid currents are harmonic-free. RSC is controlled for achieving maximum power point tracking (MPPT) and also for making unity power factor at the stator side using voltage-oriented reference frame. Synchronous reference frame (SRF) control method is used for extracting the fundamental component of load currents for the GSC control.

III. DESIGN OF DFIG-BASED WECS

Selection of ratings of VSCs and dc-link voltage is very much important for the successful operation of WECS. The ratings of DFIG and dc machine used in this experimental system are given in Appendix. In this section, a detailed design of VSCs and dc-link voltage is discussed for the experimental system used in the laboratory.

A. Selection of DC-Link Voltage

Normally, the dc-link voltage of VSC must be greater than twice the peak of maximum phase voltage. The selection of dc link voltage depends on both rotor voltage and PCC voltage. While considering from the rotor side, the rotor voltage is slip times the stator voltage. DFIG used in this prototype has stator to rotor turns ratio as 2:1. Normally, the DFIG operating slip is ± 0.3 . So, the rotor voltage is always less than the PCC voltage. So, the design criteria for the selection of dc-link voltage can be achieved by considering only PCC voltage. While considering

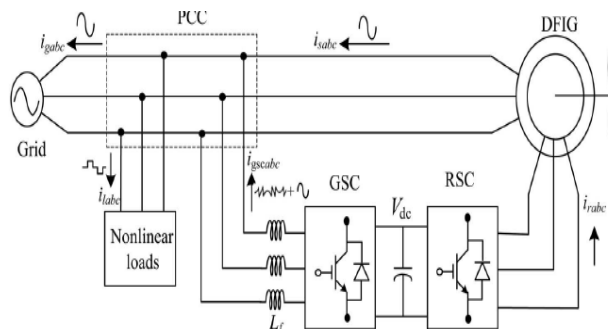


Fig. 1. Proposed system configuration.

from the GSC side, the PCC line voltage (v_{ab}) is 230 V, as the machine is connected in delta mode. Therefore, the dc-link voltage is estimated as [31]

$$V_{dc} \geq \frac{2\sqrt{2}}{\sqrt{3} * m} V_{ab} \quad (1)$$

Where V_{ab} is the line voltage at the PCC. Maximum modulation index is selected as 1 for linear range. The value of dc-link voltage (V_{dc}) by (1) is estimated as 375 V. Hence, it is selected as 375 V.

B. Selection of VSC Rating

The DFIG draws a lagging volt-ampere reactive (VAR) for its excitation to build the rated air gap voltage. It is calculated from the machine parameters that the lagging VAR of 2 kVAR is needed when it is running as a motor. In DFIG case, the operating speed range is 0.7 to 1.3 p.u. Therefore, the maximum slip (s_{max}) is 0.3. For making unity power factor at the stator side, reactive power of 600 VAR ($s_{max} * Q_s = 0.3 * 2 \text{ kVAR}$) is needed from the rotor side (Q_{rmax}). The maximum rotor active power is ($s_{max} * P$). The power rating of the DFIG is 5 kW. Therefore, the maximum rotor active power (P_{rmax}) is 1.5 kW ($0.3 * 5 \text{ kW} = 1.5 \text{ kW}$). So, the rating of the VSC used as RSC

S rated is given as

$$S_{rated} = \sqrt{P_{rmax}^2 + Q_{rmax}^2} \quad (2)$$

Thus, kVA rating of RSC S_{rated} is calculated as 1.615 kVA.

C. Design of Interfacing Inductor

The design of interfacing inductors between GSC and PCC depends upon allowable GSC current limit (i_{gscpp}), dc-link voltage, and switching frequency of GSC. Maximum possible GSC line currents are used for the calculation. Maximum line current depends upon the maximum power and the line voltage at GSC. The maximum possible power in the GSC is the slip power. In this case, the slip power is 1.5 kW. Line voltage (V_L) at the GSC is 230 V (the machine is connected in delta mode). So, the line current is obtained as $I_{gsc} = 1.5 \text{ kW} / (\sqrt{3} * 230) = 3.765 \text{ A}$. Considering the peak ripple current as 25% of rated GSC current, the inductor value is calculated as

$$L_i = \frac{\sqrt{3} m V_{dc}}{12 a f_m \Delta i_{gsc}} = \frac{\sqrt{3} * 1 * 375}{12 * 1.5 * 10000 * 0.25 * 3.76} = 3.8 \text{ mH} \quad (3)$$

Interfacing inductor between PCC and GSC is selected as 4 mH.

IV. PROPOSED FLC CONTROL STRATEGY

Control algorithms for both GSC and RSC are presented in this section. Complete control schematic is given in Fig. 2. The control algorithm for emulating wind turbine characteristics using dc machine and Type A chopper is also shown in Fig. 2.

A. Control of RSC

The main purpose of RSC is to extract maximum power with independent control of active and reactive powers. Here, the RSC is controlled in voltage-oriented reference frame. Therefore, the active and reactive powers are controlled by controlling direct and quadrature axis rotor currents (i_{dr} and i_{qr}), respectively. Direct axis reference rotor current is selected such that maximum power is extracted for a particular wind speed. This can be achieved by running the DFIG at a rotor speed for a particular wind speed. Therefore, the outer loop is selected as a speed controller for achieving direct axis reference rotor current (i_{dr}^*) as $i_{dr}^*(k) = i_{dr}^*(k-1) + k_{ipd} \{ \omega_{er}(k) - \omega_{er}(k-1) \} + k_{id} \omega_{er}(k)$ (4)

where the speed error (ω_{er}) is obtained by subtracting sensed speed (ω_r) from the reference speed (ω^*r). k_{pd} and k_{id} are the proportional and integral constants of the speed controller. $\omega_{er}(k)$ and $\omega_{er}(k-1)$ are the speed errors at k th and $(k-1)$ th instants. $i_{dr}^*(k)$ and $i_{dr}^*(k-1)$ are the direct axis rotor reference current at k th and $(k-1)$ th instants. Reference rotor speed (ω^*r) is estimated by optimal tip speed ratio control for a particular wind speed.

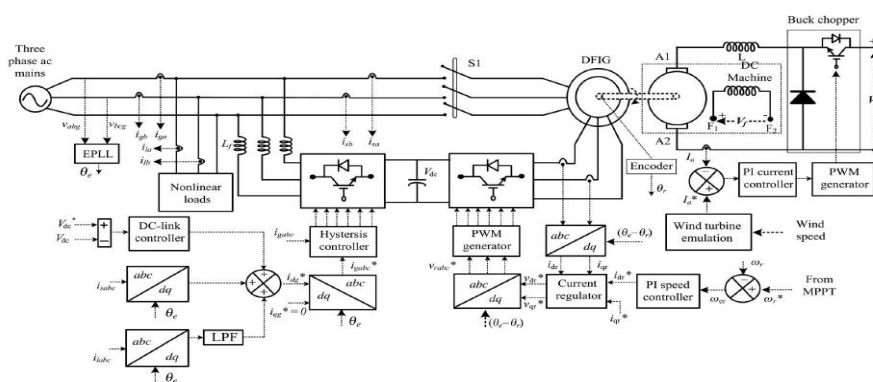


Fig. 2. Control algorithm of the proposed WECS.

The tuning of PI controllers used in both RSC and GSC are achieved using Ziegler Nichols method. Initially, k_{id} value is set to zero and the value of k_{pd} was increased until the response starts oscillating with a period of T_i . Now, the value of k_{pd} is taken as $0.45 k_{pd}$ and k_{id} is taken as $1.2 k_{pd}/T_i$. Normally, the quadrature axis reference rotor current (i_{qr}^*) is selected such that the stator reactive power (Q_s) is made zero. In this DFIG, quadrature axis reference rotor current (i_{qr}^*) is selected for injecting the required reactive power. Inner current control loops are taken for control of actual direct and quadrature axis rotor currents (i_{dr} and i_{qr}) close to the direct and quadrature axis reference rotor currents (i_{dr}^* and i_{qr}^*). The rotor currents i_{dr} and i_{qr} are calculated from the sensed rotor currents (i_{ra} , i_{rb} , and i_{rc}) as [32]

$$i_{dr} = \frac{2}{3} \begin{bmatrix} i_{ra} \sin \theta_{slip} + i_{rb} \sin (\theta_{slip} - 2\pi/3) \\ + i_{rc} \sin (\theta_{slip} + 2\pi/3) \end{bmatrix} \quad (5)$$

$$i_{qr} = \frac{2}{3} \begin{bmatrix} i_{ra} \cos \theta_{slip} + i_{rb} \cos (\theta_{slip} - 2\pi/3) \\ + i_{rc} \cos (\theta_{slip} + 2\pi/3) \end{bmatrix} \quad (6)$$

where slip angle (θ_{slip}) is calculated as

$$\theta_{slip} = \theta_e - \theta_r \quad (7)$$

where θ_e is calculated from PLL for aligning rotor currents into voltage axis. The rotor position (θ_r) is achieved with an encoder. Direct and quadrature axis rotor voltages (v_{dr} and v_{qr}) are obtained from direct and quadrature axis rotor current errors (i_{dr} and i_{qr}) as

$$v'_{qr}(k) = v'_{qr}(k-1) + k_{pqr} \{i_{qer}(k) - i_{qer}(k-1)\} + k_{iqv} i_{qer}(k) \quad (8)$$

Where

$$i_{der} = i_{dr}^* - i_{dr} \text{ and } i_{qer} = i_{qr}^* - i_{qr} \quad (9)$$

where k_{pdr} and k_{idr} are the proportional and integral gains of direct axis current controller. k_{pqr} and k_{iqv} are the proportional and integral gains of quadrature axis current controller. Direct and quadrature components are decoupled by adding some compensating terms as [26]

$$v_{dr}^* = v'_{dr} + (\omega_e - \omega_r) \sigma L_r i_{qr} \quad (10)$$

$$v_{qr}^* = v'_{qr} - (\omega_e - \omega_r) (L_m i_{ms} + \sigma L_r i_{dr}) \quad (11)$$

These reference direct and quadrature voltages (v^*_{dr} , v^*_{qr}) are converted into three phase reference rotor voltages

(v^*_{ra} , v^*_{rb} , v^*_{rc}) as [32]

$$v_{ra}^* = v_{dr}^* \sin \theta_{slip} + v_{qr}^* \cos \theta_{slip} \quad (12)$$

$$v_{rb}^* = v_{dr}^* \sin(\theta_{slip} - 2\pi/3) + v_{qr}^* \cos(\theta_{slip} - 2\pi/3) \quad (13)$$

$$v_{rc}^* = v_{dr}^* \sin(\theta_{slip} + 2\pi/3) + v_{qr}^* \cos(\theta_{slip} + 2\pi/3) \quad (14)$$

These three phase rotor reference voltages (v_{ra} , v_{rb} , v_{rc}) are compared with triangular carrier wave of fixed switching frequency for generating pulse-width modulation (PWM) signals for the RSC.

B. Control of GSC

The novelty of this work lies in the control of this GSC for mitigating the harmonics produced by the nonlinear loads. The control block diagram of GSC is shown in Fig. 2. Here, an indirect current control is applied on the grid currents for making them sinusoidal and balanced. Therefore, this GSC supplies the harmonics for making grid currents sinusoidal and balanced. These grid currents are calculated by subtracting the load currents from the summation of stator currents and GSC currents. Active power component of GSC current is obtained by processing the dc-link voltage error (v_{dce}) between reference and estimated dc-link voltage (V^*_{dc} and V_{dc}) through PI controller as

$$i_{gsc}^*(k) = i_{gsc}^*(k-1) + k_{pdc} \{v_{dce}(k) - v_{dce}(k-1)\} + k_{idc} v_{dce}(k) \quad (15)$$

where k_{pdc} and k_{idc} are proportional and integral gains of dc-link voltage controller. $v_{dce}(k)$ and $v_{dce}(k-1)$ are dc-link voltage errors at k th and $(k-1)$ th instants. $i_{gsc}^*(k)$ and $i_{gsc}^*(k-1)$ are active power component of GSC current at k th and $(k-1)$ th instants. Active power component of stator current (i_{ds}) is obtained from the sensed stator currents (i_{sa} , i_{sb} , and i_{sc}) using abc to dq transformation as [32]

$$i_{ds} = 2/3 [i_{sa} \sin \theta_e + i_{sb} \sin(\theta_e - 2\pi/3) + i_{sc} \sin(\theta_e + 2\pi/3)] \quad (16)$$

Fundamental active load current (i_{ld}) is obtained using SRF theory [33]. Instantaneous load currents (i_{labc}) and the value of phase angle from EPLL are used for converting the load currents in to synchronously rotating dq frame (i_{ld}). In synchronously rotating frames, fundamental frequency currents are converted into dc quantities and all other harmonics are converted into non-dc quantities with a frequency shift of 50 Hz. DC values of load currents in synchronously rotating dq frame (i_{ld}) are extracted using low-pass filter (LPF). Direct axis component of reference grid current (i^*_{gd}) is obtained from the direct axis current of stator current (i_{ds}) and load current (i_{ld}) in synchronously rotating frame and the loss component of GSC current (i^*_{gsc}) as

$$i_{gd}^* = i_{gsc}^* + i_{ds} - \overline{i_{ld}} \quad (17)$$

Quadrature axis component of reference grid current (i_{gq}^*) is selected as zero for not to draw any reactive power from grid. Reference grid currents (i_{ga}^* , i_{gb}^* , and i_{gc}^*) are calculated from the direct and quadrature axis grid currents (i_{gd}^* , i_{gq}^*) [32]. The hysteresis current controller is used to generate switching pulses for the GSC. The hysteresis controller is a feedback current control where sensed current tracks the reference current within a hysteresis band (i_{hb}) [34]. At every sampling instant, the actual current (i_{gabc}) is compared to the reference current (i_{gabc}^*) as

$$\Delta i_{gabc} = i_{gabc}^* - i_{gabc} \quad (18)$$

when $\Delta i_{gabc} > i_{hb}$, lower switch is turned ON (19)

when $\Delta i_{gabc} < -i_{hb}$, upper switch is turned ON. (20)

Using these equations, gating pulses for three phases of GSC are generated in the same way.

The fuzzy logic controller unlike conventional controllers does not require a mathematical model of the system process being controlled. However, an understanding of the system process and the control requirements is necessary. The fuzzy controller designs must define what information data flows into the system (control input variable), how the information data is processed (control strategy and decision) and what information data flows out of the system (solution output variables) [16]. In this study, a fuzzy logic based feedback controller is employed for controlling the voltage injection of the proposed dynamic voltage restorer (DVR). Fuzzy logic controller is preferred over the conventional PI and PID controller because of its robustness to system parameter variations during operation and its simplicity of implementation [17]. The proposed FLC scheme exploits the simplicity of the mamdani type fuzzy systems that are used in the design of the controller and adaptation mechanism.

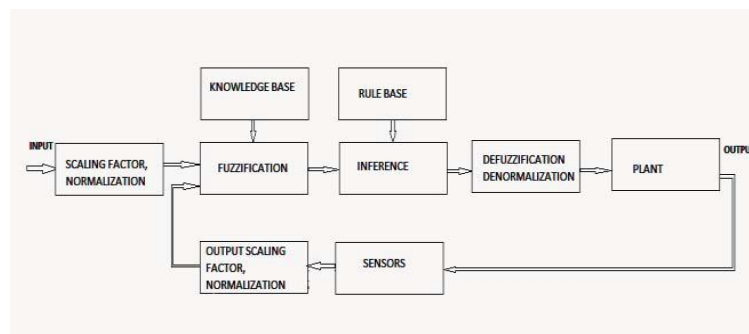


Figure 3: Fuzzy logic controller

The fuzzy logic control scheme (shown in figure 3) can be divided into four main functional blocks namely knowledge base, fuzzification, inference mechanism and defuzzification. The knowledge base is composed of database and rule base. Data base consists of input and output membership functions and provides information for appropriate fuzzification and defuzzification operations. The rule base consists of a set of linguistic rules relating the fuzzified input variables to the desired control actions. Fuzzification converts a crisp input voltage signals, error voltage signal (e) and change in error voltage signal (ce) into fuzzified signals that can be identified by level of memberships in the fuzzy sets. The inference mechanism uses the collection of linguistic rules to convert the input conditions of fuzzified outputs to crisp control conditions using the output membership function, which in the system acts as the changes in the control input (u).

'e'	NB	NM	NS	ZE	PS	PM	PB
'ce'							
NB	NB	NB	NB	NB	NM	NS	ZE
NM	NB	NB	NB	NM	NS	ZE	PS
NS	NB	NB	NM	NS	ZE	PS	PM
ZE	NB	NM	NS	ZE	PS	PM	PB
PS	NM	NS	ZE	PS	PM	PB	PB
PM	NS	ZE	PS	PM	PB	PB	PB
PB	ZE	PS	PM	PB	PB	PB	PB

Table 2: Rule base for fuzzy logic controller

The set of fuzzy control linguistic rules is given in table 2. The inference mechanism in fuzzy logic controller utilizes these rules to generate the required output.

V. MATLAB RESULTS AND DISCUSSION

MATLAB/SIMULINK results are presented in this section for validating steady-state and dynamic performances of this proposed DFIG with integrated active filter capabilities.

In this section, the working of this proposed GSC is presented as an active filter even when the wind turbine is in shutdown condition. The power that is coming into the PCC through GSC is considered as positive in this paper.

In this section, the working of this proposed GSC is presented as an active filter even when the wind turbine is in shutdown condition. The power that is coming into the PCC through GSC is considered as positive in this paper.

The simulated performance of this proposed DFIG is presented at a 10.6-m/s wind speed as shown in Fig. 4. As the proposed DFIG is operating at MPPT, the reference speed of the DFIG is selected as 1750 rpm. The load currents are observed to be nonlinear in nature. The GSC is supplying required harmonics currents to the load for making grid currents ($igabc$) and stator currents ($isabc$) balanced and sinusoidal. Fig. 4 also shows the stator power (Ps), GSC power ($Pgsc$), load power (Pl), and grid power (Pg). At above synchronous speed, the power flow is from the GSC to PCC, so the GSC power is shown as positive. Total power produced by the DFIG is the sum of stator power (Ps) and GSC power ($Pgsc$). After feeding power to the load (Pl), the remaining power is fed to the grid (Pg). Fig. 5 (a)–(d) shows harmonic spectra and waveforms of grid current (iga), load current (ila), stator current (isa), and grid voltage (vga), respectively. From these harmonic spectra, one can understand that grid current and stator current THDs are less than 5% as per IEEE-519 standard [35] limits given in Table I. Fig. 5 shows test results by performing tests on the developed prototype at a fixed wind speed of 10.6 m/s. These test results are observed similar to the simulated results.

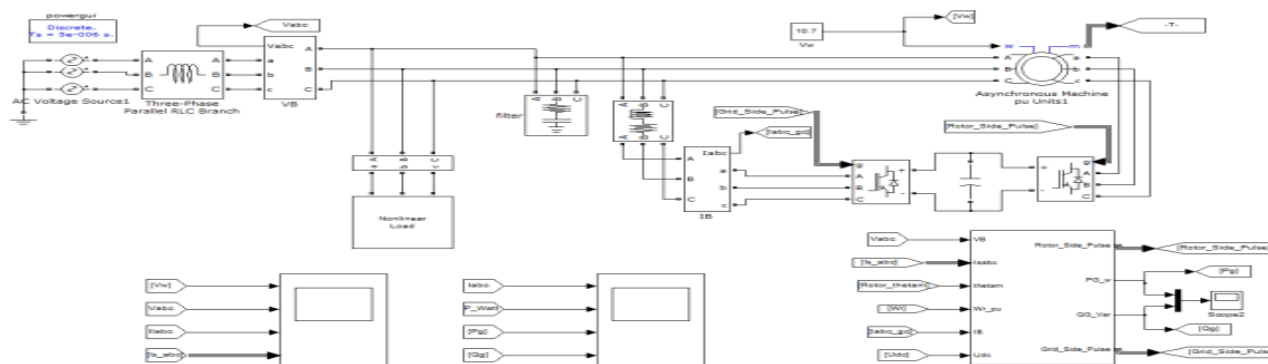


Fig 4. MATLAB SIMULINK Model of the Proposed DFIG

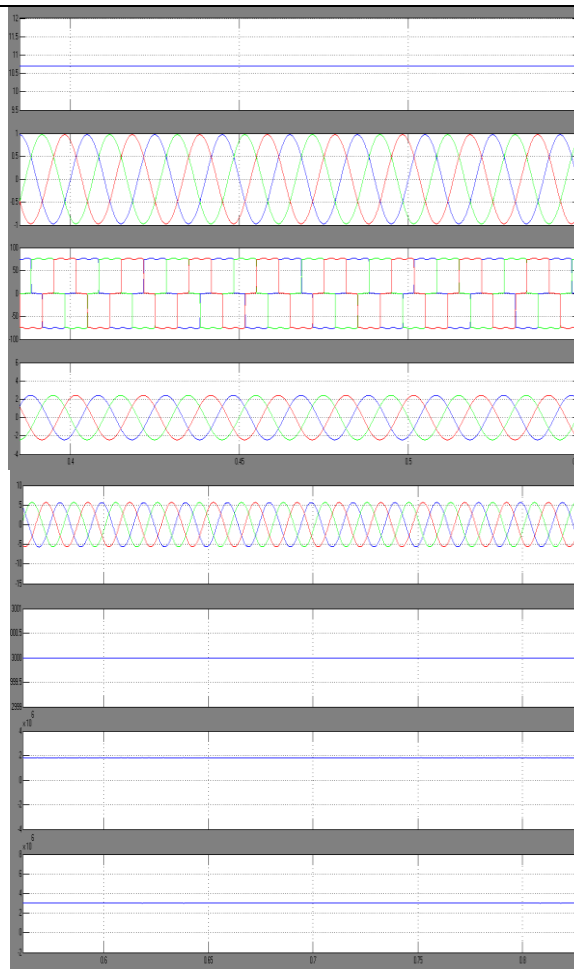


Fig. 5. Simulated performance of the proposed DFIG-based WECS at fixed wind speed of 10.6 m/s (rotor speed of 1750 rpm).

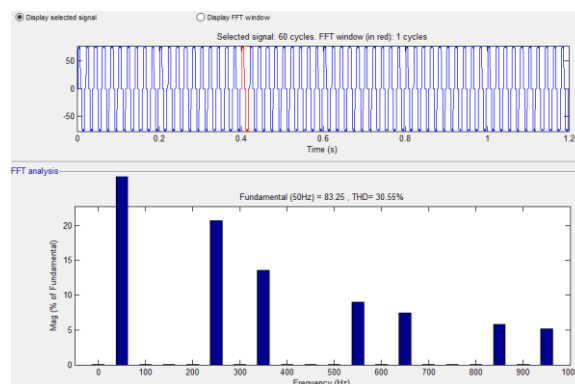


Fig 6 Total Harmonic Distortion of Load current (I_{labc}) in %

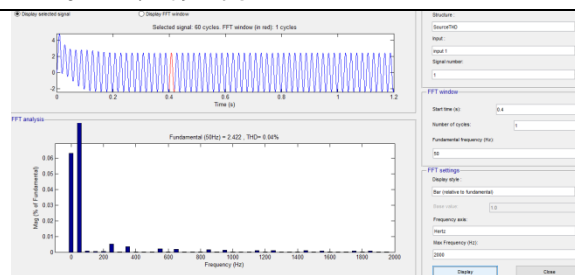


Fig 7 Total Harmonic Distortion of Source current(Isabc) in %

VI. CONCLUSION

The FLC based GSC control algorithm of the proposed DFIG has been modified for supplying the harmonics and reactive power of the local loads. In this proposed Fuzzy Logic control based DFIG, the reactive power for the induction machine has been supplied from the RSC and the load reactive power has been supplied from the GSC. The decoupled control of both active and reactive powers has been achieved by RSC control. The proposed FLC based DFIG has also been verified at wind turbine stalling condition for compensating harmonics and reactive power of local loads. This proposed FLC DFIG-based WECS with an integrated active filter has been simulated using MATLAB/Simulink environment, and the simulated results are verified with test results of the developed prototype of this WECS. Steady-state performance of the proposed DFIG has been demonstrated for a wind speed. Dynamic performance of this proposed Fuzzy Logic control has also been verified for the variation in the wind speeds and for local nonlinear load.

REFERENCES

- [1]. D. M. Tagare, *Electric Power Generation the Changing Dimensions*. Piscataway, NJ, USA: IEEE Press, 2011.
- [2]. G. M. Joselin Herbert, S. Iniyar, and D. Amutha, "A review of technical issues on the development of wind farms," *Renew. Sustain. Energy Rev.*, vol. 32, pp. 619–641, 2014.
- [3]. I. Munteanu, A. I. Bratcu, N.-A. Cutululis, and E. Ceang, *Optimal Control of Wind Energy Systems Towards a Global Approach*. Berlin, Germany: Springer-Verlag, 2008.
- [4]. A. A. B. Mohd Zin, H. A. Mahmoud Pesaran, A. B. Khairuddin, L. Jahanshaloo, and O. Shariati, "An overview on doubly fed induction generators controls and contributions to wind based electricity generation," *Renew. Sustain. Energy Rev.*, vol. 27, pp. 692–708, Nov. 2013.
- [5]. S. S. Murthy, B. Singh, P. K. Goel, and S. K. Tiwari, "A comparative study of fixed speed and variable speed wind energy conversion systems feeding the grid," in *Proc. IEEE Conf. Power Electron. Drive Syst. (PEDS'07)*, Nov. 27–30, 2007, pp. 736–743.
- [6]. D. S. Zinger and E. Muljadi, "Annualized wind energy improvement using variable speeds," *IEEE Trans. Ind. Appl.*, vol. 33, no. 6, pp. 1444–1447, Nov./Dec. 1997.
- [7]. H. Polinder, F. F. A. van der Pijl, G. J. de Vilder, and P. J. Tavner, "Comparison of direct-drive and geared generator concepts for wind turbines," *IEEE Trans. Energy Convers.*, vol. 21, no. 3, pp. 725–733, Sep. 2006.
- [8]. R. Datta and V. T. Ranganathan, "Variable-speed wind power generation using doubly fed wound rotor induction machine—A comparison with alternative schemes," *IEEE Trans. Energy Convers.*, vol. 17, no. 3, pp. 414–421, Sep. 2002.
- [9]. E. Muljadi, C. P. Butterfield, B. Parsons, and A. Ellis, "Effect of variable speed wind turbine generator on stability of a weak grid," *IEEE Trans. Energy Convers.*, vol. 22, no. 1, pp. 29–36, Mar. 2007.
- [10]. R. Pena, J. C. Clare, and G. M. Asher, "Doubly fed induction generator using back-to-back PWM converters and its application to variable-speed wind-energy generation," *IEE Proc. Elect. Power Appl.*, vol. 143, no. 3, pp. 231–241, May 1996.
- [11]. S. Muller, M. Deicke, and R. W. De Doncker, "Doubly fed induction generator systems for wind turbines," *IEEE Ind. Appl. Mag.*, vol. 8, no. 3, pp. 26–33, May/Jun. 2002.
- [12]. W. Qiao and R. G. Harley, "Grid connection requirements and solutions for DFIG wind turbines," in *Proc. IEEE Energy 2030 Conf. (ENERGY'08)*, Nov. 17–18, 2008, pp. 1–8.
- [13]. A. Petersson, T. Thiringer, L. Harnefors, and T. Petru, "Modeling and experimental verification of grid interaction of a DFIG wind turbine," *IEEE Trans. Energy Convers.*, vol. 20, no. 4, pp. 878–886, Dec. 2005.

- [14]. H.M. Hasanien, "Aset-membership affine projection algorithm-based adaptive-controlled SME Sunits for wind farms output power smoothing," *IEEE Trans. Sustain. Energy*, vol.5,no.4,pp.1226–1233,Oct.2014.
- [15]. Z.Saad-Saoud,M.L.Lisboa, J.B.Ekanayake, N.Jenkins,andG.Strbac, "Application of STATCOM stowindfarms," *IEEProc.Gener.Transmiss.Distrib.*, vol.145,no.5,pp.511–516,Sep.1998.
- [16]. G.O.SuvireandP.E.Mercado,"Combinedcontrolofadistribu-tionstaticsynchronouscompensator/flywheelenergystoragesystemfor windenergyapplications,"*IETGener.Transmiss.Distrib.*,vol.6,no.6,pp.483–492,Jun.2012.
- [17]. D. Somayajula and M. L. Crow, "An ultra capacitor integrated power conditioner for intermittency smoothing and improving power quality of distribution grid," *IEEE Trans. Sustain. Energy*, vol. 5, no. 4, pp. 1145–1155, Oct. 2014.
- [18]. M. T. Abolhassani, P. Enjeti, and H. Toliyat, "Integrated doubly fed electrical alternator/active filter (IDEA), a viable power quality solution, for wind energy conversion systems," *IEEE Trans. Energy Convers.*, vol. 23,no. 2, pp. 642–650, Jun. 2008.
- [19]. A. Gaillard, P. Poure, and S. Saadate, "Active filtering capability of WECS with DFIG for grid power quality improvement," in *Proc. IEEE Int. Symp. Ind. Electron.*, Jun. 30, 2008, pp. 2365–2370.
- [20]. A. Gaillard, P. Poure, and S. Saadate, "Reactive power compensation and active filtering capability of WECS with DFIG without any overrating," *Wind Energy*, vol. 13, pp. 603–614, 2009.
- [21]. M. Boutoubat, L. Mokrani, and M. Machmoum, "Control of a wind energy conversion system equipped by a DFIG for active power generation and power quality improvement," *Renew. Energy*, vol. 50, pp. 378–386, Feb. 2013.
- [22]. A. Ejlali and D. Arab Khaburi, "Power quality improvement using nonlinear-load compensation capability of variable speed DFIG based on DPC-SVM method," in *Proc. 5th Power Electron. Drive Syst. Technol. Conf. (PEDSTC)*, Feb. 5–6, 2014, pp. 280–284.
- [23]. B. Mohamed, L. Mokrani, and M. Machmoum, "Full capability of harmonic current mitigation for a wind energy system," *Elect. Power Comp. Syst.*, vol. 42, no. 15, pp. 1743–1753, 2009.
- [24]. E. Tremblay, A. Chandra, and P. J. Lagace, "Grid-side converter control of DFIG wind turbines to enhance power quality of distribution network," in *Proc. IEEE PES Gen. Meeting*, 2006, p. 6.
- [25]. E. Tremblay, S. Atayde, and A. Chandra, "Direct power control of a DFIG-based WECS with active filter capabilities," in *Proc. IEEE Elect. Power Energy Conf. (EPEC)*, Oct.22–23,2009,pp.1–6.
- [26]. G. Todeschini and A. E. Emanuel, "Wind energy conversion system as an active filter: Design and comparison of three control systems," *IET Renew. Power Gener.*, vol. 4, no. 4, pp. 341–353, Jul. 2010.
- [27]. B. N. Singh, A. Chandra, and K. Al-Haddad, "Performance comparison of two current control techniques applied to an active filter," in *Proc. 8th Int. Conf. Harmonics Qual. Power Proc.*, Oct. 14–18, 1998, vol. 1, pp. 133–138.
- [28]. B. N. Singh, A. Chandra, and K. Al-Haddad, "DSP-based indirect current-controlled STATCOM. I. Evaluation of current control techniques," *IEE Proc. Elect. Power Appl.*, vol. 147, no. 2, pp. 107–112, Mar. 2000.
- [29]. B. N. Singh, A. Chandra, and K. Al-Haddad, "DSP-based indirect current- controlled STATCOM. II. Multifunctional capabilities," *IEE Proc. Elect. Power Appl.*, vol. 147, no. 2, pp. 113–118, Mar.2000.
- [30]. B. N. Singh, B. Singh, A. Chandra, P. Rastgoufard, and K. Al-Haddad, "An improved control algorithm for active filters," *IEEE Trans. Power Del.*, vol. 22, no. 2, pp. 1009–1020, Apr. 2007.
- [31]. S. Sharma and B. Singh, "Voltage and frequency control of asynchronous generator for stand-alone wind power generation," *IET Power Electron.*, vol. 4, no. 7, pp. 816–826, Aug. 2011.
- [32]. G. Abad, J. López, M. Rodríguez, L. Marroyo, and G. Iwanski, *Doubly Fed Induction Machine: Modeling and Control for Wind Energy Generation Applications*. Hoboken, NJ, USA: Wiley/IEEE Press,2011.
- [33]. B. Singh and J. Solanki, "A comparison of control algorithms for DSTATCOM," *IEEE Trans. Ind. Elect.*, vol. 56, no. 7, pp. 2738–2745, Jul. 2009.
- [34]. B. K. Bose, *Modern Power Electronics and AC Drives*, 4th ed. Englewood Cliffs, NJ, USA: Prentice-Hall, 2007, ch. 5.
- [35]. *IEEE Recommended Practices and Requirements for Harmonic Control in Electrical Power Systems*, IEEE Standard 519, 1992.
- [36]. *Electrical Power Systems* (6th edition) by C.L.Wadhwa.
- [37]. *Electrical Conersion Systems* (3rd edition) by Raokash Das Begumudre.